Hydrophobe-Water Interactions: Methane as a Model

F. Despa*† and R. S. Berry†‡
*Department of Pharmacology, University of California, Davis, California; and †Department of Chemistry and ‡James Franck Institute, University of Chicago, Chicago, Illinois

ABSTRACT Recent molecular-dynamics simulations have demonstrated that the use of an empirical hydrophobic potential displaying two minima, i.e., one for hydrophobes in close contact and one for hydrophobes separated by a hydration layer, leads to a marked improvement in protein structure prediction. This potential is supported by experimental data and simulations, but its physical origin and mathematical formulation have not been derived as yet. Here we show that water-mediated attraction (the "wetting regime") between two hydrophobic molecules originates in the interaction between the dipoles induced at the surface of the hydrophobes by the surrounding structured water. As an example, we derive the effective hydrophobic potential that describes the interaction between two methane molecules, a classical model of a double-well energy function. We found an excellent agreement with published results from all-atom, explicit solvent molecular-dynamics simulations of this interaction. The approach presented here provides the theoretical basis for implementing an adequate representation of the wetting regime of the hydrophobic interactions in force fields used for structure prediction. The results are useful for modeling both protein folding and binding.

INTRODUCTION

In proteins, the key requirements for a successful folding process are achieving the unique folded shape and maintaining the ability to change conformation (1). Folding in the native structure is central to protein function (2), whereas preserving sufficient structural mobility prevents proteins from getting stuck in local energy minima (1). Apparently, this delicate balance between the rigidity and flexibility of the protein structure is maintained by an adequate number of intramolecular hydrogen bonds (HBs) and hydrophobic interactions with in the surrounding water (3–15). On one hand, intramolecular HBs that may increase the rigidity of protein structures can easily be transferred to surrounding water molecules (4). On the other hand, a too-lax molecular structure will regain stability by making additional backbone HBs and wrapping them with hydrophobic groups to keep water away (5). Water molecules are also involved in tuning the strength of the hydrophobic interactions between nonpolar side chains of the protein (9,14,15), thus enabling optimal rearrangements of the hydrophobic core in the final, native state (6,7,16).

Because water molecules play an active role in protein folding (for a recent review, see Ball 17), increasing efforts being directed toward searching for adequate representations of the solvent in models for structure prediction. An explicit atomistic description of the surrounding water in MD simulations of protein folding remains computationally very expensive (6,7,16,18–20), restricting the timescales and conformational space that can be accessed. Therefore, the use of potential functions to describe water-mediated interactions between protein structural units remains particularly appealing for modeling protein folding and binding. Previous molecular-dynamics (MD) simulations with an implicit solvent in the energy function (10,13) suggested that long-range water-mediated potentials guide folding and smooth the underlying folding funnel. Apparently, surrounding water molecules promote long-range pairing of hydrophilic groups and facilitate native-like packing of structural units. Much in the same manner, water molecules can foster an interaction between otherwise noninteracting hydrophobes (9,14). The polarization field created by water structured at the surface of the hydrophobic groups can induce long-range attractions between two such surfaces. Experimental data and computer simulations (21–25) support the idea that the hydrophobic interaction relevant for protein folding is within the wetting regime, where hydrophobic groups can interact at distances outside the van der Waals range. These data motivated the introduction of an empirical hydrophobic potential, the hydrophobic potential of mean force (HPMF), to describe the interaction of the hydrophobic groups in the wetting regime (15,26). In combination with Lennard-Jones (LJ) 6-12 short-ranged interaction terms, this effective potential displays two minima: one for hydrophobes in close contact, and one for hydrophobes separated by a hydration layer (15). Recent MD simulations demonstrated that the effective hydrophobic potential with two minima leads to a marked improvement in protein structure prediction (15).

The ad hoc introduction of the second minimum (15) in the hydrophobic energy function is physically motivated by experimental data and MD simulations (21–25), and, a posteriori, is justified by an excellent performance in structure prediction (15). The physical origin and mathematical formulation of the second potential well of the HPMF energy function has not been derived as yet. Here, we use basic molecular principles to show that the physical origin of the second potential well of the HPMF energy function (15) is due to the interaction between the dipoles induced at the surface of the hydrophobes by the surrounding polarized water (9). This induced dipole-dipole interaction is attractive in nature and

Submitted May 10, 2008, and accepted for publication July 29, 2008.

Address reprint requests to F. Despa. E-mail: fdespa@ucdavis.edu.

Editor: Gregory A. Voth.

0006-3495/08/11/4241/05 $2.00

doi: 10.1529/biophysj.108.137216

long-ranged, i.e., for small systems, it scales with r^{-3}, where r is the distance between the interacting hydrophobes (14). The r^{-3} term describes the precursor (wetting) regime of the hydrophobic interaction that occurs before the entropy increase that results from releasing the water layers, and the short-range van der Waals attraction provides the driving force to ''dry out'' the contact surface. By moving the hydrophobes closer, the r^{-3} contribution to the effective hydrophobic potential vanishes due to the depletion of the water layers between the two interacting hydrophobes, leaving in place only the LJ 6-12 short-range interaction terms (Fig. 1). Consequently, the effective potential displays two minima separated by a barrier at a critical distance between the two interacting hydrophobes. The position of the barrier depends on the distribution profile of the correlated water molecules in between the hydrophobic groups. To illustrate this phenomenon, we derive here the effective hydrophobic potential that describes the interaction between two methane molecules. We found an excellent agreement with the results of all-atom, explicit solvent MD simulations reported by Rick and Berne (27). The approach presented here provides the theoretical basis for implementing an adequate representation of the wetting regime of the hydrophobic interactions in force fields used for structure prediction. The results are useful for modeling both protein folding and binding.

MATERIALS AND METHODS

The wetting regime of hydrophobic attractions

Water is characterized by a random, fluctuating, three-dimensional network of HBs (28). The exchange of HBs between water molecules is associated with a fast and arbitrary reorientation of their individual molecular dipoles ($\vec{d}$) under the influence of the thermal energy. The highest mobility of $\vec{d}$ in the environment is determined by an entirely balanced exchange of HBs in all directions. At the interface between water and a non-H-bonding solute, water molecules have fewer opportunities for the H-bond exchange, leading to apparent orientational ordering (29–31) and extended lag times for reorientation of the dipole moments (9). The retardation of the relaxation dynamics of water molecular dipoles at the surface gives rise to coupling and correlation between them, generating persistent polarization fields. The polarization field of correlated water will induce a dipole at the hydrophobic surface (14) and subsequent induced dipole-dipole interactions between hydrophobic surfaces approaching one another. Therefore, hydrophobic aggregation begins with a step in which nonpolar solutes approach one another due to long-range electrostatic forces (the wetting regime).

In our previous work (9,14) we presented a self-consistent molecular approach describing how water molecules organize themselves around hydrophobic units and give rise to polarization fields that can set effective long-range attractions between hydrophobic units. According to this theory, the overall average interaction energy between two identical (nonrigid) hydrophobic units in the wetting regime results in an attractive energy term varying as r^{-3} of the form (14)

$$u_{\mathrm{h}}(r) = -\left(\frac{\gamma}{l^3}\right)^2 \frac{2d^2}{4\pi\varepsilon_0}\left(\frac{N_0}{f}\overline{\langle\vec{\mu}\rangle}\right)^2 \frac{1}{r^3}. \qquad (1)$$

Here, ε_0 stands for the dielectric constant of the vacuum, r represents the instantaneous distance between the interacting hydrophobic units, γ denotes the polarizability of the hydrophobic molecule and l is its characteristic length, and $\langle\vec{\mu}\rangle$ stands for the thermodynamic average of the water molecular dipole moment $\vec{d}$, i.e., $\langle\vec{d}\rangle = d\langle\vec{\mu}\rangle$. In deriving Eq. 1, we kept in mind that the vector dipole field $\vec{E}$ at each site in the correlated region is a random variable, and consequently $\langle\vec{\mu}\rangle$ must be averaged over the probability of distribution of the internal field $\vec{E}$ (9). Therefore, $\overline{\langle\vec{\mu}\rangle}$ in Eq. 1 is the mean value of the water molecular dipole in the internal field $\vec{E}$ of all the other water molecular dipoles in the correlated region. This is a function of temperature (T) and a parameter f measuring the depletion of the exchanging HBs, relative to bulk water, in dipole-dipole correlated water, $\overline{\langle\vec{\mu}\rangle} = \overline{\langle\vec{\mu}(T,f)\rangle}$ (9). N_0 represents the number of molecular dipoles in a domain that extends over a distance

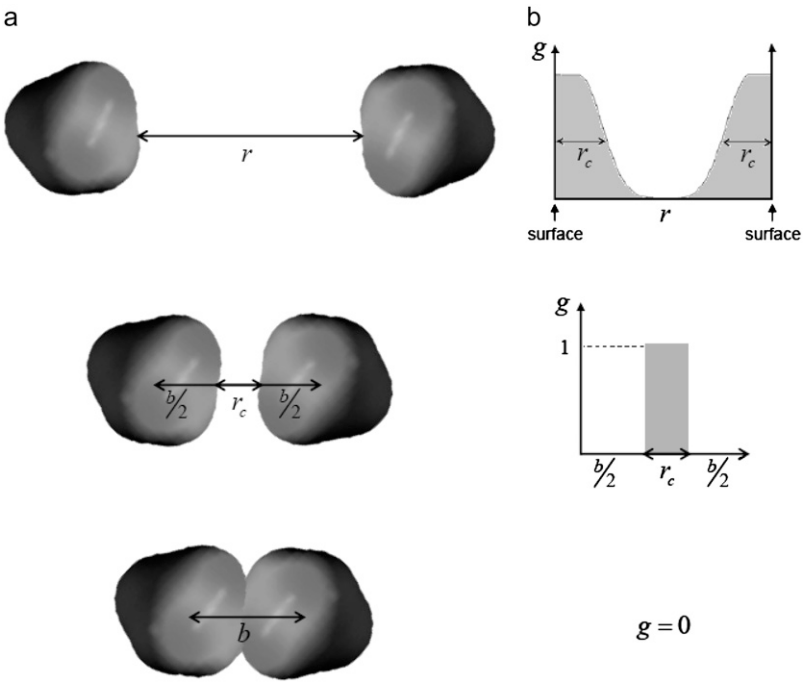

FIGURE 1 (*a*) Diagram suggesting the hydrophobic interaction in the wetting regime. At a separation distance between hydrophobes of about r_c, most of the water molecular dipoles in between the two surfaces are strongly correlated. However, moving the hydrophobes closer drives the water out, so that when they meet and direct contacts form between the surfaces, all correlated waters are expelled. (*b*) Distribution profile $g(r)$ of correlated water molecular dipoles confined between the two hydrophobic surfaces corresponding to *a*.

r_c from the hydrophobic surface, $N_0 \cong (ASA\, r_c/v_0)$, where ASA is the accessible area of the hydrophobic surface delineating the domain, and v_0 is the volume of a water molecule. r_c is derived from equilibrium energy consideration by considering that the stability of the molecular dipole pairs in the domain of correlated water is provided by the interplay between the dipole pairwise interaction and the entropy change, as shown previously (9), $r_c \cong a_0[1+(1/3\beta E_L d)\ln(m/(m-f))]$. Here, a_0 is the characteristic interspace between two water molecules in bulk, m is the number of HBs per water molecules in bulk water, β has the usual meaning $(\beta = (1/k_B T))$, and E_L is the Lorentz field, $E_L = (dn/3\varepsilon_0)$, with n standing for the typical number density of bulk water.

At a separation distance between hydrophobes of about $r \cong b + r_c$ (Fig. 1), most of the water molecular dipoles in between the two surfaces are strongly correlated, producing the highest polarization field and subsequently the strongest induced dipole-dipole interaction. However, moving the hydrophobes closer drives the water out, so that when they meet and direct contacts form between the surfaces, all correlated waters are expelled (12,32–34). According to the above description, the effective potential energy (U_h) describing the association of two hydrophobic groups approaching one another can be written (when f is nonzero) as

$$U_h(r) = w_0\left[\left(\frac{b}{r}\right)^{12} - 2\left(\frac{b}{r}\right)^{6}\right] - \left(\frac{\gamma}{l^3}\right)^2 \frac{2d^2}{4\pi\varepsilon_0} \times \left(\frac{ASA\, r_c}{v_0 f}\, g(r)\overline{\langle\vec{\mu}\rangle}\right)^2 \frac{1}{r^3}. \quad (2)$$

Here $g(r)$, in the second term of the equation, represents the specific distribution profile of the correlated water molecular dipoles between the two surfaces. Thus, the maximum number of water molecular dipoles in correlated states occurs when the two neighboring hydrophobic surfaces are separated by a linear distance r_c (9), which renders $g = 1$ at $r \cong b + r_c$ (Fig. 1 *b*). For $r < b + r_c$, water molecules correlated in pairs are rapidly depleted, leading to $g = 0$, at $r \cong b$. Therefore, the r^{-3} contribution to $U_h(r)$ vanishes at $r \cong b$, leaving in place only the short-range interaction contributions. These short-range forces are represented by the LJ 6-12 potential in the first term of Eq. 2. w_0 and b are the characteristic parameters of this potential.

RESULTS AND DISCUSSION

The second term of Eq. 2 describes the wetting regime of the hydrophobic attraction. We can observe that the strength of this attraction depends on the effective dipole moment ($\overline{\langle\vec{\mu}\rangle}$) of water correlated at the interface (9) and geometries of the hydrophobic molecules. The dependence on molecular geometries includes explicit terms, such as surface areas (ASA), characteristic lengths (l), and polarizabilities (γ). In addition, the hydrophobic attraction depends on the depletion parameter f, which is an implicit function of the shape of the hydrophobic molecule (i.e., $f = 3$ corresponds to water molecules rotationally immobilized by hydrophobic interfaces, $f = 2$ is appropriate for describing water molecules at planar interfaces, and $f = 1$ characterizes small hydrophobic species (14)). By looking at Eq. 2, we can see that large values of the depletion parameter f can lead to a fast decrease in the strength of the long-range hydrophobic attraction. Large values of f are also associated with a local reduction of the density of water molecules (9), which drop the polarization field associated with correlated waters to low values and lower the strength of interaction. Hence, the depth of the potential well describing the wetting regime of the hydrophobic interaction is the result of a subtle balance between the size and shape of the hydrophobic surface.

Because $\overline{\langle\vec{\mu}\rangle}$ decreases at high temperatures (14), thermal agitation can be sufficient to overcome the long-range hydrophobic attraction ($u_h \to 0$ for $\beta E_L d \ll 80$). Thus the attraction between the two hydrophobes corresponding to the wetting regime is typically low in comparison with usual electrostatic forces ($(u_h/E_L d) < 1$). However, in the range of temperatures of biological interest ($\beta E_L d \cong 80$), the hydrophobic attraction generated by polarized water can be sufficiently strong to keep nonpolar molecules together.

As an example, we used Eq. 2 to derive the effective hydrophobic potential that describes the interaction between two methane molecules, for which $\gamma = 2.70\,\text{Å}^3$ and $l = 3.7\,\text{Å}$ (35), at $T = 300\,\text{K}$. The parameters for the LJ 6-12 potential are: $w_0 = 0.38\,\text{Kcal mol}^{-1}$ and $b = 3.7\,\text{Å}$ (35). Within this computation, we assumed a distribution profile $g(r)$ of the correlated water molecular dipoles confined between the two hydrophobic surfaces as displayed in Fig. 1 *b*. The other parameters used in the computation are: $a_0 = 2.8\,\text{Å}$, $d = 1.8\,D$, $ASA = \pi\,(l)^2$, $f = 1$, and $m = 4$. The mean value of the water molecular dipole ($\overline{\langle\vec{\mu}\rangle}$) in the correlated region at $T = 300\,\text{K}$ (i.e., $\beta E_L d = 80$) and $f = 1$ is $\overline{\langle\vec{\mu}\rangle} \cong 0.2$ (14). As expected, the resulted effective potential displays two minima (Fig. 2), i.e., one corresponding to the interaction between methane molecules in the wetting regime and one for molecules in close contact. The position of the barrier between potential wells depends on the distribution profile of water correlated at the interface, $N_0\, g(r)$.

From Fig. 2 we can observe that, to strengthen the interaction, water molecules must leave the thin layer separating the two hydrophobes. This corresponds to a transition from the wetting regime to direct contact between molecules. This

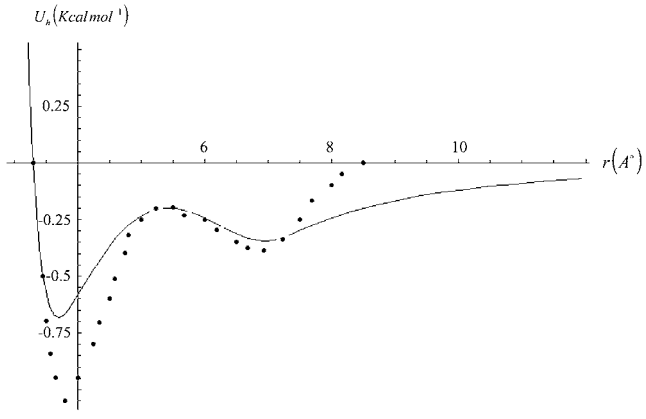

FIGURE 2 The effective hydrophobic potential that describes the interaction of two methane molecules computed with the proposed approach (see Eq. 2). The parameters for the LJ 6-12 potential are: $w_0 = 0.38\,\text{Kcal mol}^{-1}$ and $b = 3.7\,\text{Å}$ (35). The other parameters used in the computation are: $\gamma = 2.70\,\text{Å}^3$ (35), $l = 3.7\,\text{Å}$ (35), $a_0 = 2.8\,\text{Å}$, $T = 300\,\text{K}$, $d = 1.8\,D$, $ASA = \pi\,(l)^2$, $f = 1$ and $m = 4$. For comparison, we also plotted (as points) part of the results of Rick and Berne (27) at $T = 298\,\text{K}$.

shows that within the classical model of dry hydrophobic surfaces in contact at equilibrium (36), the forces that bind hydrophobes together can perfectly well be all the van der Waals contacts between them. But those forces have a short range, and they cannot account for why the hydrophobes ever want to come together. The interaction mechanism described by Eq. 2 gives the long-range potential that induces them to approach one another. Then, when they are very close, the entropy of releasing the water layers (8,12,32,33), and of course the van der Waals attractions, may well provide enough driving force to dry out the contact surface.

The effective hydrophobic potential obtained in this approach is in very good agreement with the methane pair potential of mean force derived from all-atom, explicit solvent MD simulations reported by Rick and Berne (27). Both positions and relative depths of the minima are similar for the two potentials. However, a noticeable difference can be observed in the region corresponding to the very long-range interaction ($r > r_c + b$). The effective hydrophobic potential obtained in the approach presented here shows that the attraction between methane molecules would start at longer distances than that revealed by MD simulations. This difference may arise in part from the use in the MD simulations of the fluctuating charge model (37). Typically, the fluctuating charge model neglects the dipole polarizability contribution to the energy of interaction between molecules. It is worth noting at this point, however, that most hydrophobic amino acids have significant polarizabilities (38). Therefore, the induced dipole-dipole contribution may need to be adequately considered in estimating the overall interaction energy (15).

MD simulations of the hydrophobic effect performed by Lin et al. (39) assumed a model in which the hydrophobic walls were rigid and nonpolarizable. A large variety of force fields (SPC, SPCE, TIP3P, TIP4P, and TIP5P) used in MD simulations of the hydrophobic effect were calibrated to reproduce mainly the water density curves (see, for instance, the critical review by Paschek (40)). It seems that the developers of these codes paid less attention to secondary effects, such as induced dipole-dipole interactions produced by the polarization field of caged water. Recent MD simulations (41) revealed that polarizability plays an important role in determining the hydrophobic force that acts between nonrigid, hydrophobic surfaces in water, as we suggested earlier (9,14). Nonlinear electrostatic contributions to the energy transfer from water to hydrophobic environments are also likely to play an important role in setting the local equilibrium of the system (42). Based on these results (9,14,41,42), one can expect the correlation effects of water molecules confined between extended weakly polar surfaces to differ significantly from those observed in water caged between rigid hydrophobic walls (39). According to the results presented here and those published earlier (14), contributions from induced dipole-dipole interactions can explain the effective long-range attraction measured between extended hydrophobic surfaces in water, as reported by several previous studies (43–45).

CONCLUSIONS

The nonmonotonic behavior beyond the energy minimum corresponding to hydrophobic species in close contact may have various sources, including packing of water molecules around each of the interacting atoms (46), charge transfer between the first hydration layer and hydrophobic molecules (27,37) and dispersion-induction effects due to water structuring in between the hydrophobes (9,14). Apparently, complete drying is not essential to promote an attractive interaction between hydrophobic, weakly polarizable solutes. Attractions between such species were predicted from both basic molecular principles (9,14) and MD simulations (41,47). Direct measurements also revealed long-range attractive forces between hydrophobic surfaces in water (43–45). In this work, we have shown that hydrophobes can actually attract each other at separation distances much larger than those typically used in computing van der Waals energies. Here we have shown that the physical origin of the state of water-mediated attraction is the interaction between the dipoles induced at the surface of the hydrophobes by the surrounding polarized water. The long-range interaction part of the effective hydrophobic potential obtained within this approach describes very well the behavior of nonpolar solutes in a wetting regime of the type used by Lin et al. (15) for protein structure prediction.

The approach presented here provides the theoretical basis for implementing an adequate representation of the wetting regime of the hydrophobic interactions in force fields used for structure prediction. Long-range hydrophobic interactions in the wetting regime may ensure a better flexibility of the domains in forming a near-native structure of the protein structure and may increase the dynamics in the configuration space (1). Nonetheless, we can infer from these results that nonpolar residues behave differently in the presence of interstitial water compared with how they interact when buried in a dried protein core. Therefore, water may be the lubricant that enables the hydrophobic core of a protein to reach its optimally packed state (6,7,16). The results presented here are useful for modeling both protein folding and binding.

F.D. thanks the John von Neumann Institute for Computing, Research Centre Jülich, where much of this work was done, for its hospitality. R.S.B. acknowledges the hospitality of the Aspen Center for Physics, where some of his contribution to this work was carried out.

REFERENCES

1. Frauenfelder, H., S. G. Sligar, and P. G. Wolynes. 1991. The energy landscapes and motions of proteins. *Science*. 254:1598–1603.
2. Anfinsen, C. B. 1973. Principles that govern folding of protein chains. *Science*. 181:223–230.

3. Dill, K. A. 1990. Dominant forces in protein folding. *Biochemistry*. 29:7133–7155.
4. Mattos, C., and D. Ringe. 2001. Proteins in organic solvents. *Curr. Opin. Struct. Biol.* 11:761–764.
5. Fernandez, A., and R. S. Berry. 2002. Extent of hydrogen-bond protection in folded proteins: a constraint on packing architectures. *Biophys. J.* 83:2475–2481.
6. Shea, J. E., J. N. Onuchic, and C. L. Brooks 3rd. 2002. Probing the folding free energy landscape of the Src-SH3 protein domain. *Proc. Natl. Acad. Sci. USA*. 99:16064–16068.
7. Garcia, A. E., and J. N. Onuchic. 2003. Folding a protein in a computer: an atomic description of folding/unfolding of protein A. *Proc. Natl. Acad. Sci. USA*. 100:13898–13903.
8. Huang, X., C. J. Margulis, and B. J. Berne. 2003. Dewetting-induced collapse of hydrophobic particles. *Proc. Natl. Acad. Sci. USA*. 100: 11953–11958.
9. Despa, F., A. Fernandez, and R. S. Berry. 2004. Dielectric modulation of biological water. *Phys. Rev. Lett.* 93:228104.
10. Papoian, G. A., J. Ulander, M. P. Eastwood, Z. Luthey-Schulten, and P. G. Wolynes. 2004. *Proc. Natl. Acad. Sci. USA*. 101:3352–3357.
11. Chandler, D. 2005. Interfaces and the driving force of hydrophobic assembly. *Nature*. 437:640–647.
12. Liu, P., X. Huang, R. Zhou, and B. J. Berne. 2005. Observation of a dewetting transition in the collapse of the melittin tetramer. *Nature*. 437:159–162.
13. Zong, C., G. A. Papoian, J. Ulander, and P. G. Wolynes. 2006. Role of topology, nonadditivity, and water-mediated interactions in predicting the structures of α/β proteins. *J. Am. Chem. Soc*. 128:5168–5176.
14. Despa, F., and R. S. Berry. 2007. The origin of the long-range attraction of hydrophobes in water. *Biophys. J*. 92:373–378.
15. Lin, M. S., N. L. Fawzi, and T. Head-Gordon. 2007. Hydrophobic potential of mean force as a salvation function for protein structure prediction. *Structure*. 15:727–740.
16. Cheung, M. S., A. E. Garcia, and J. N. Onuchic. 2002. Protein folding mediated by salvation: water expulsion and formation of the hydrophobic core occur after the structural collapse. *Proc. Natl. Acad. Sci. USA*. 99:685–690.
17. Ball, P. 2008. Water as an active constituent in cell biology. *Chem. Rev*. 108:74–108.
18. Duan, Y., and P. A. Kollman. 1998. Pathways to a protein folding intermediate observed in a 1-microsecond simulation in aqueous solutions. *Science*. 282:740–744.
19. Mirny, L., and E. Shakhnovich. 2001. Protein folding theory: from lattice to all-atom models. *Annu. Rev. Biophys. Biomol. Struct*. 30:361–396.
20. Daggett, V., and A. Fersht. 2003. The present view of the mechanism of protein folding. *Nat. Rev. Mol. Cell Biol*. 4:497–502.
21. Head-Gordon, T., J. M. Sorenson, A. Pertsemlidis, and R. M. Glaeser. 1997. Differences in hydration structure near hydrophobic and hydrophilic amino acids. *Biophys. J*. 73:2106–2115.
22. Hura, G., J. M. Sorenson, R. M. Glaeser, and T. Head-Gordon. 1999. Solution X-ray scattering as a probe of hydration-dependent structuring of aqueous solutions. *Perspect. Drug Discov. Des*. 17:97–118.
23. Pertsemlidis, A., A. M. Saxena, A. K. Soper, T. Head-Gordon, and R. M. Glaeser. 1996. Direct evidence for modified solvent structure within the hydration shell of a hydrophobic amino acid. *Proc. Natl. Acad. Sci. USA*. 93:10769–10774.
24. Pertsemlidis, A., A. K. Soper, J. M. Sorenson, and T. Head-Gordon. 1999. Evidence for microscopic, long-range hydration forces for a hydrophobic amino acid. *Proc. Natl. Acad. Sci. USA*. 96:481–486.
25. Sorenson, J. M., G. Hura, A. K. Soper, A. Pertsemlidis, and T. Head-Gordon. 1999. Determining the role of hydration forces in protein folding. *J. Phys. Chem. B*. 103:5413–5426.
26. Crivelli, S., E. Eskow, B. Bader, V. Lamberti, R. Byrd, R. Schnabel, and T. Head-Gordon. 2002. A physical approach to protein structure prediction. *Biophys. J*. 82:36–49.
27. Rick, S. W., and B. J. Berne. 1997. Free energy of the hydrophobic interaction from molecular dynamics simulations: the effect of solute and solvent polarizability. *J. Phys. Chem. B*. 101:10488–10493.
28. Sceats, M. G., and S. A. Rice. 1982. Water: A Comprehensive Treatise. Vol. 7. F. Franks, editor. Plenum Press, New York.
29. Frank, H. S., and M. W. Evans. 1945. Free volume and entropy in condensed systems III. entropy in binary liquid mixtures; partial molal entropy in dilute solutions; structure and thermodynamics in aqueous electrolytes. *J. Chem. Phys*. 13:507–532.
30. Blokzijl, W., and J. B. F. N. Engberts. 1993. Hydrophobic effects. Opinions and facts. *Angew. Chem. Int. Ed. Engl*. 32:1545–1579.
31. Jensen, M. Ø., O. G. Mouritsen, and G. H. Peters. 2004. The hydrophobic effect: molecular dynamics simulations of water confined between extended hydrophobic and hydrophilic surfaces. *J. Chem. Phys*. 120: 9729–9744.
32. Pangali, C., M. Rao, and B. J. Berne. 1979. Monte-Carlo simulation of the hydrophobic interaction. *J. Chem. Phys*. 71:2975–2980.
33. Lum, K., D. Chandler, and J. D. Weeks. 1999. Hydrophobicity at small and large length scales. *J. Phys. Chem. B*. 103:4570–4577.
34. ten Wolde, P. R., and D. Chandler. 2002. Drying-induced hydrophobic polymer collapse. *Proc. Natl. Acad. Sci. USA*. 99:6539–6543.
35. Graziano, G. 1998. On the size dependence of hydrophobic hydration. *J. Chem. Soc., Faraday Trans*. 94:3345–3352.
36. Kauzmann, W. 1959. Some factors in the interpretation of protein denaturation. *Adv. Protein Chem*. 14:1–63.
37. Rick, S. W., S. J. Stuart, and B. J. Berne. 1994. Dynamical fluctuating charge force fields: application to liquid water. *J. Chem. Phys*. 101: 6141–6156.
38. Chipot, C., B. Maigret, J. L. Rivail, and H. A. Scheraga. 1992. Determination of net atomic charges from ab initio self-consistent-field molecular electrostatic properties. *J. Phys. Chem*. 96:10276–10284.
39. Lee, C. Y., J. A. McCammon, and P. J. Rossky. 1984. The structure of liquid water at an extended hydrophobic surface. *J. Chem. Phys*. 80:4448–4455.
40. Paschek, D. 2004. Temperature dependence of the hydrophobic hydration and interaction of simple solutes: an examination of five popular water models. *J. Chem. Phys*. 120:6674–6690.
41. Bresme, F., and A. Wynveen. 2007. On the influence of solute polarizability on the hydrophobic interaction. *J. Chem. Phys*. 126:044501.
42. Gong, H., G. Hocky, and K. F. Freed. 2008. Influence of nonlinear electrostatics on transfer energies between liquid phases: charge burial is far less expensive than Born model. *Proc. Natl. Acad. Sci. USA*. In press.
43. Pashley, R. M., P. M. McGuiggan, B. Ninham, and D. F. Evans. 1985. Attractive forces between uncharged hydrophobic surfaces: direct measurements in aqueous solution. *Science*. 229:1088–1089.
44. Tsao, Y.-H., D. F. Evans, and H. Wennerström. 1993. Long-range attractive force between hydrophobic surfaces observed by atomic force microscope. *Science*. 262:547–550.
45. Meyer, E. E., Q. Lin, T. Hassenkam, E. Oroudjev, and J. N. Israelachvili. 2005. Origin of the long-range attraction between surfactant-coated surfaces. *Proc. Natl. Acad. Sci. USA*. 102:6839–6842.
46. Pettitt, B. M., and M. Karplus. 1985. The potential of mean force surface for the alanine dipeptide in aqueous solution: a theoretical approach. *Chem. Phys. Lett*. 121:194–201.
47. Choudhury, N., and B. M. Pettitt. 2007. The dewetting transition and the hydrophobic effect. *J. Am. Chem. Soc*. 129:4847–4852.